SL2

REAL-TIME TRACKING OF FAST SUPERPARAMAGNETIC NANOPARTICLE SELF-ASSEMBLING BY FOCUSED SYNCHROTRON BEAM

M. Jergel[1], P. Šiffalovič[1], E. Majková[1], L. Chitu[1], Š. Luby[1], I. Capek[2], A. Šatka[3], A. Timmann[4], S. V. Roth[4]

[1]*Institute of Physics, Slovak Academy of Sciences, Dúbravská cesta 9, 84511 Bratislava, Slovakia*
[2]*Polymer Institute, Slovak Academy of Sciences, Dúbravská cesta 9, 84236 Bratislava, Slovakia*
[3]*International Laser Center, Ilkovičova 3, 81219 Bratislava, Slovakia*
[4]*HASYLAB/DESY, Notkestrasse 86, 22603 Hamburg, Germany*
matej.jergel@savba.sk

Latest advances in nanochemistry made possible the synthesis of highly monodisperse colloidal nanoparticles. In particular, magnetic nanoparticles become increasingly important in applied materials science (bio-applications, emerging spintronic devices, etc.). Well correlated nanoparticle templates result from the process of spontaneous nanoparticle self-assembly which is a fast and cost effective way of fabrication of nanoparticle monolayers. Here we report on a real time observation of the spontaneous self-assembly process of superparamagnetic Fe_3O_4 nanoparticles in a fast drying colloidal drop by grazing-incidence small-angle X-ray scattering (GISAXS). The experiments were conducted at BW4 beamline at HASYLAB. The focused X-ray beam of the size 65 35 m^2 and the wavelength of 0.138 nm hits a silicon substrate at 0.2 grazing angle of incidence. The X-ray camera PILATUS 100K with the read-out time of 3 ms between subsequent frames and the pixel size of 172 172 m^2 was used at a distance of 225 cm from the sample. The exposure time of a frame was set to 25 ms. The colloidal drop was applied manually on the silicon substrate. The zero of the time scale is related to the activation of the hutch interlocks and has some 30 s delay with respect to the drop application. In these measurements, the absolute time scale is not relevant. To relate time evolution of the reciprocal space and direct space features and to localize the nanoparticle self-assembling, vertical or horizontal sample oscillations were applied (Fig. 1).

In the first stage after application, the drop wets the substrate and the drop contact line reaches its maximum diameter. The second stage is dominated by a linear decrease of the drop mass accompanied by a shrinking of the drop contact line. The nanoparticles serve as pinning centers which can be observed as a gradual *stick-slip* motion of the drop contact line. The third stage starts when the evaporation-driven surface tension instability initiates random drop movement along the substrate. In this study, we addressed mainly the second evaporation stage that is responsible for self-assembling. In the zone Z0 (Fig. 1), the sampling beam is located above the drop surface and only a background scattering is recorded. The limits of the zone Z1 are defined by the first contacts of the beam with the drop surface and the substrate. Here, the scattering is due solely to the drop near-surface region and drop volume. The zone Z2 produces a combined scattering by the drying drop and the substrate. The zone Z1 plays the major role in this study since it gives an unambiguous determination of

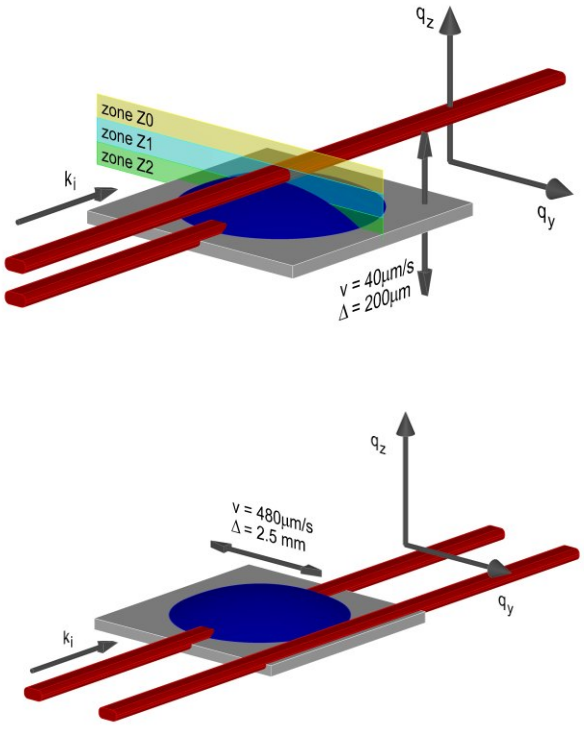

Figure 1. Vertical (top) and horizontal (bottom) scanning schemes.

the scattering volume. The GISAXS pattern recorded after a complete solvent evaporation exhibits side maxima at q_y 0.82 nm^{-1} produced by the self assembled nanoparticle areas and a central streak along q_z at $q_y = 0$ coming from the substrate and nanoparticle-related roughness which is usually measured in the q_x q_z plane (coplanar geometry) as a detector scan. The GISAXS pattern simulated within the DWBA and paracrystal model provided nanoparticle radius of 3.4 ± 0.3 nm, interparticle distance of 7.5 ± 1 nm, and lateral correlation length of 87 nm.

The data from time-resolved GISAXS taken on the oscillating sample were processed into two different kinds of maps (Fig. 2). In a so called t q_y map, the region between $q_z = 0.22$ and 0.4 nm^{-1} was integrated and plotted as a function of time. In a so called t q_z map, integration for q_y be-

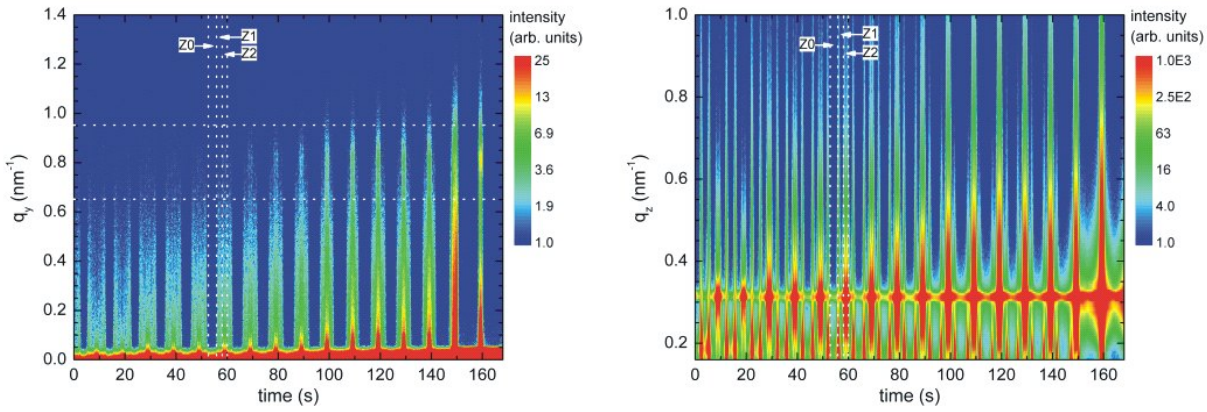

Figure 2. The t - q_y and t - q_z maps of the drying colloidal drop forming a monolayer in the vertical scanning mode.

tween ±0.02 nm^{-1} was performed and plotted as a function of time. Briefly, the t q_y map describes the temporal evolution of the q_y component of the scattering vector near the critical exit angle and the t q_z map describes the temporal evolution of what is called above the detector scan. The instances when the sampling X-ray beam comes into contact with the drop surface (Z0 Z1 transition) or when it leaves the drop (Z1 Z0 transition) are clearly visible as an enhanced scattering along q_y direction in the t q_y map for the early evaporation stage (less than 60 s). In between, more absorbed and weaker radiation coming from the zone Z2, where the X-ray beam starts to interact with the substrate, can be seen. The Z0 Z1 and Z1 Z0 transitions are marked also by significant scattering in the t q_z map while the detector scans in between produced by the substrate scattering in the zone Z2 are less prominent. This behaviour is reversed at later evaporation stages (more than 60 s) where the main scattering stems from the zone Z2 and the substrate scattering plays the major role. It can be observed in the t q_y map as a strong scattering signal surrounded by a lower one coming from the zone Z1. Similarly in the t q_z map, the detector scans resulting from the Z0 Z1 and Z1 Z0 transitions are decreasing in intensity in favour of the detector scans originating from the substrate scattering in the zone Z2. The temporal approaching of the occurrence of the detector scans (i.e. Z0 Z1 and Z1 Z0 transitions) belonging to one sample oscillation cycle indicates the thinning of the evaporating colloidal drop. Similar temporal plots related to different sample regions can be drawn from the integration of the subsequent GISAXS frames over the square regions around the side maxima and specular reflection. All these analyses imply that the self assembly starts in the vicinity of the drop contact line rather than near the surface or inside the drop. This is in line with our previous observations where no self-assembled clusters were found with measurements in a so called *drop mode* where the incoming beam parallel to the substrate surface probed only the drop volume [1].

To support the assumption about the self-assembling near the contact line, we employed also a horizontal scanning scheme as shown in Fig. 1. Here, the sample oscillates horizontally across the incoming X-ray beam which intersects periodically the shrinking drop contact line during the solvent evaporation. The scanning velocity was adapted to the exposure and read-out times of the X ray camera in order to minimize the effect of the spatial smearing on the scattering volume sampled by the X ray beam. The t q_y map measured in the horizontal scanning mode is shown in Fig. 3a. At the beginning, periodic stripes of an enhanced intensity along the q_y axis with the maximum at q_y 0.82 nm^{-1} coming from the already dried regions of the self assembled monolayer of nanoparticles and adjacent low-absorbing volume of the drop close to the three-phase contact line, are observed.

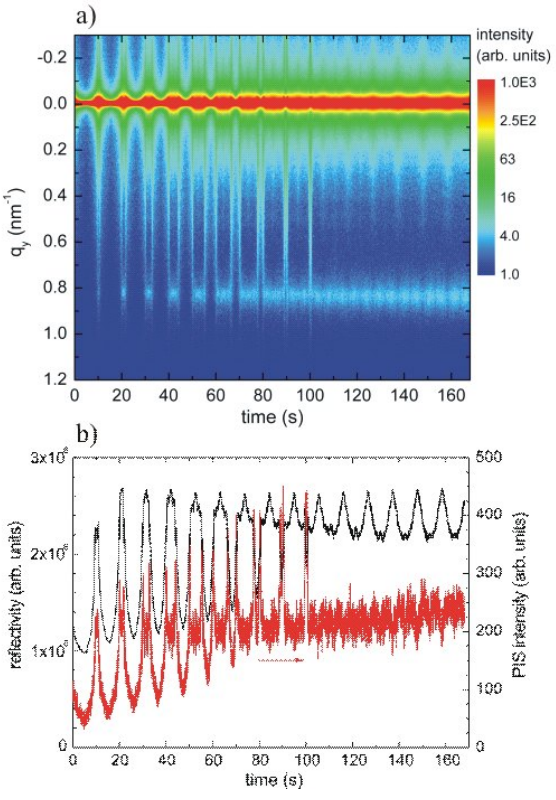

Figure 3. The t - q_y map (a) and time-resolved reflectivity (upper curve) and PIS (lower curve) (b) of the drying colloidal drop forming a monolayer in the horizontal scanning mode.

In between, the sampling X-ray beam enters the drop and is strongly suppressed in intensity by the drop absorption, showing no correlations between the nanoparticle positions. The peak at q_y 0.82 nm^{-1} persists up to the complete drop evaporation that indicates a well ordered and stable nanoparticle monolayer. The temporal plot extracted from the GISAXS pattern by integration over the region of the side maximum (partial integrated scattering – PIS) is compared with the time resolved specular reflectivity curve in Fig. 3b. The minima in the PIS plot and reflectivity are correlated in the early evaporation stages as both are observed when the probing x ray beam is strongly attenuated inside the drop. As the beam crosses the three-phase contact line and leaves the drop, an enhanced scattering in the PIS plot is observed, followed by a significant increase of the reflectivity signal. The opposite takes place when the beam enters the drop. The reflectivity maxima correspond to extreme positions of the horizontal scan when the maximum area of the bare substrate adjacent to the drop is hit by the probing beam. In between, the reflectivity comes mainly from the already dried areas of the colloidal solution with the nanoparticle-related roughness and is thus inherently lower. On the other hand, these areas contribute to the GISAXS signal that is at maximum in the central part of the scan (i.e. in the drop center) when the drop is evaporated completely. Therefore in the final evaporation stages, the PIS signal reaches a steady-state value with a small oscillating part which is in anti-phase with the reflectivity oscillations. Here, the oscillations in the PIS plot and reflectivity are due to a periodically changing ratio between the illuminated areas favouring reflectivity (bare substrate) and GISAXS (dried nanoparticle monolayer). These measurements indicate that behind the shrinking contact line, the self assembled monolayer is originating. Because no measurable lateral correlations of the nanoparticles near the surface or inside the drop were observed by the vertical scanning, the vicinity of the three phase drop boundary is the location of the nanoparticle accumulation and self-assembling.

1. P. Šiffalovič, E. Majková, L. Chitu, M. Jergel, Š. Luby, A. Šatka, S. V. Roth, *Phys. Rev.*, **B 76**, (2007), art.no. 195432.

SL3

STRUCTURE OF GaAs WHISKERS GROWN ON SILICON NANOWIRES

P. Klang[1], A. M. Andrews[1,2], H. Detz[1], M. Steinmaier[2], A. Lugstein[2], W. Schrenk[1], G. Strasser[3]

[1]Center for Micro- and Nanostructures, TU-Wien, Floragasse 7, Vienna, Austria
[2]Institute for Solid State Electronic, TU-Wien, Floragasse 7, Vienna, Austria
[3]The State University of New York at Buffalo, USA
klang@fke.tuwien.ac.at

The combination of silicon with III-V semiconductors could offer the benefits of both material systems producing novel structures for electronic and optoelectronic applications. We present the hetero-epitaxial growth of single crystal GaAs whiskers on silicon nanowire trunks forming structures with a 6-fold symmetry (see Fig. 1). The Si nanowires on Si (111) substrates were prepared using a low pressure chemical vapor deposition reactor and the vapor-liquid-solid growth mechanism. A 2 nm thick layer of gold was sputtered on the surface as a catalyst for silicon nanowire growth. We have grown GaAs nanowhiskers on these Si {111} nanowires using solid source molecular beam epitaxy system. The samples were analyzed by several techniques – scanning electron microscopy (SEM), photoluminescence (PL) measurements, high resolution transmission electron microscopy (HRTEM) and X-ray diffraction (XRD) analysis.

HRTEM brings us a direct view of the crystal structure in the nanocrystals. The HRTEM cross-section of the Si nanowires explains the 6-fold symmetry of the GaAs nanowhiskers observed by SEM. The nanowhiskers grow perpendicular to the six side walls of the Si nanowire trunks created by six {112} facets [1]. The growth direction of the GaAs whiskers was also investigated by HRTEM and determined to be in the [0001] direction.

SEM technique provides us the information about the length and diameter of the nanowires. The length of our Si nanowires trunks are around 2 m with a diameter determined by the Au catalyst, typically less than 100 nm. The length of the nanowhiskers grown on these nanowires depends mainly on the amount of deposited GaAs material and varies from several hundreds nm to several ěm. It could be also shown that the GaAs nanowhiskers originate from any position along the Si nanowire trunks.

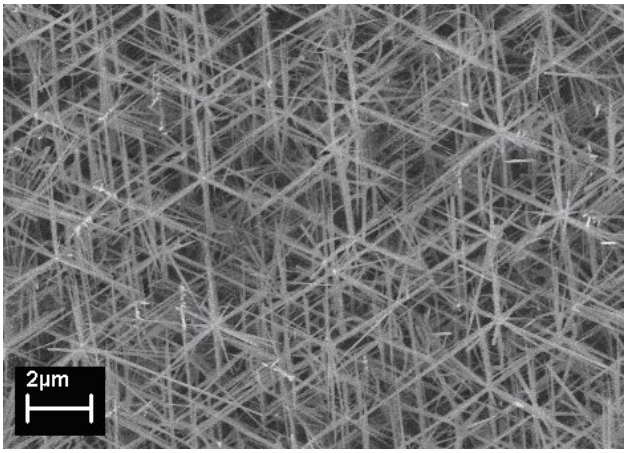

Figure 1. SEM picture of 6-fold GaAs whiskers on Si nanowire trunks visible after the deposition of 200 nm GaAs.

We used XRD to complement the TEM crystal structure analysis of our samples, with the advantage that it is non-destructive. We have measured reciprocal space maps with a wide /2 range (see Fig. 2) to find the powder dif-

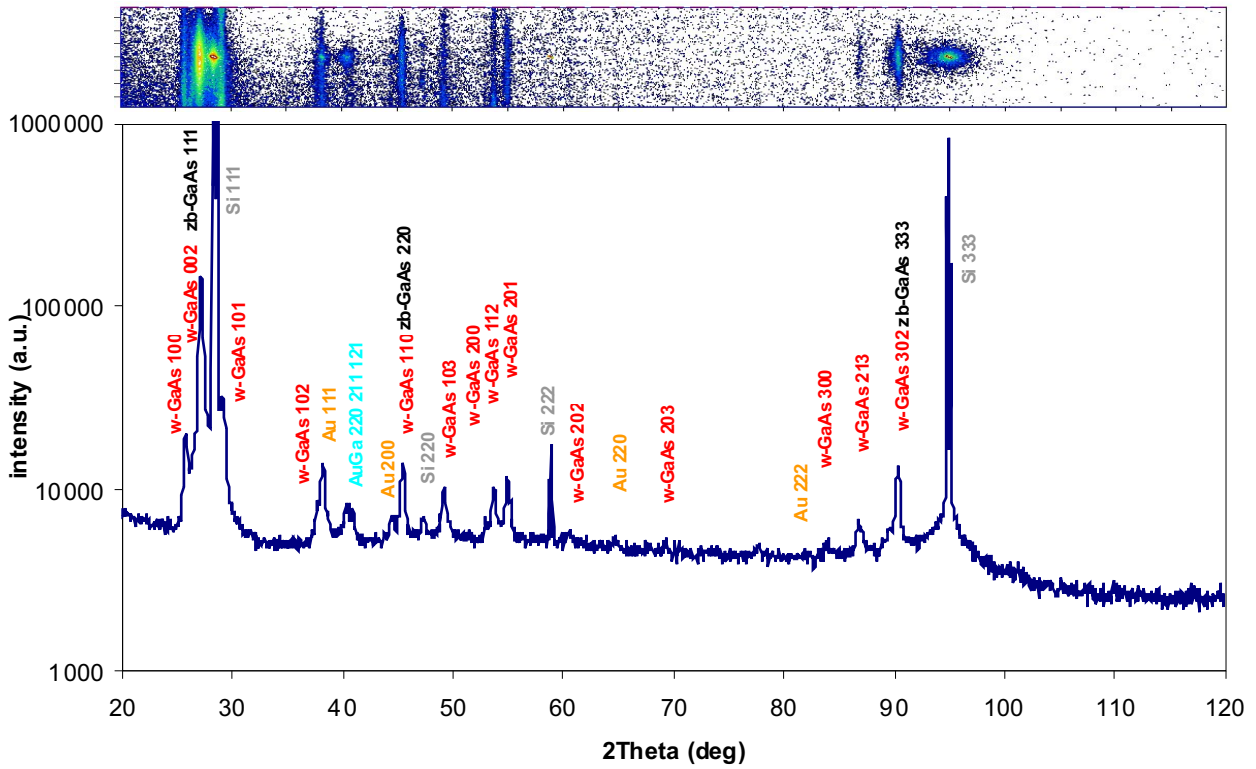

Figure 2. X-ray RSM and projection to 2 / axis measured on sample with 200 nm equivalent layer thickness of GaAs grown on silicon nanowires.

fraction peaks as well as the monocrystalline ones. The disadvantage of this method is the long measuring time required, but we obtain more information about the constituent materials. We compared different GaAs nanowhisker samples with the samples where only Si nanowires were grown to distinguish between the Si nanowire trunks and GaAs nanowhiskers. We identified monocrystalline Si, polycrystalline wurtzite GaAs, due to the distributed orientation of the single crystal nanowhiskers with respect to each other, Au and also the AuGa alloy.

We confirmed the wurtzite structure of the GaAs whiskers grown on Si nanowires by the XRD technique and additionally showed the presence of the AuGa alloy, a possible catalyst for the nanowhisker growth. The characterization of the sample structure and growth mechanism of GaAs nanowhiskers on Si nanowire trunks moves us closer to novel Si:III-V hetero-epiataxial devices.

1. A. Lugstein, A.M. Andrews, M. Steinmair, Y. Hyun, E. Bertagnolli, M. Weil, P. Ponratz, M. Schramböck, T. Roch, G. Strasser, *Nanotechnology*, **18**, (2007), 355306.

CL1

THE FIRST EXPERIENCE OF A PROTEIN CRYSTALLOGRAPHER WITH THE OXFORD DIFFRACTION ENHANCED ULTRA SOURCE AND THE ATLAS CCD DETECTOR

J. Dohnálek[1,2], T. Kovalˇ[1], M. Dušek[1]

[1]*Institute of Physics, Academy of Sciences of the Czech Republic, Cukrovarnická 10, Praha 6, Czech Republic*

[2]*Institute of Macromolecular Chemistry, Academy of Sciences of the Czech Republic, Heyrovského nám. 2, Praha 6, Czech Republic, dohnalek@fzu.cz*

The Gemini PX Ultra diffractometer with Atlas CCD detector provides a new platform for protein crystallography experiments. The enhanced copper source of X-ray radiation together with the highly sensitive CCD detector with novel features is a sufficient solution for many diffraction experiments involving single crystals of biological macromolecules.

The original design of the diffractometer with focus on "small molecule" crystallography brings many options for protein diffraction experiments not available with standard setups for macromolecular crystallography such as the kappa goniometer, possibility of non-zero theta measurements (high resolution protein diffraction with large unit cells) and variability of data collection approaches together with built-in automated design of data collection strategy.

Introductory measurements and comparative studies regarding the performance of the CCD detector with high sensitivity, dynamic range and fast readout were performed with several protein samples. Diffraction data sets of high quality were collected, including those of the extracellular part of the human receptor CD69 and other study targets. This experimental setup offers a viable option for in-house diffraction experiments with protein samples. Interestingly, protein diffraction data with the total $R_{int} < 0.03$ up to the diffraction limit of 2.0 Å have been recorded and processed.

The work was supported by the Czech Science Foundation, project No. 305/07/1073 and by the European commission, project LSHG-CT-2006-031220..